

# Design of Magnetic Blood Cleansing Microdevices through Experimentally Validated CFD Modeling

J. Gómez-Pastora<sup>1</sup>, C. González-Fernández<sup>1</sup>, I.H. Karamelas<sup>2,3</sup>, E. Bringas<sup>1</sup>, E.P. Furlani<sup>2,4</sup> and I. Ortiz<sup>1</sup>

<sup>1</sup>Dept. of Chemical and Biomolecular Engineering, University of Cantabria (Spain), gomezjp@unican.es

<sup>2</sup>Dept. Chemical and Biological Engineering, State University of New York at Buffalo (USA), efurlani@buffalo.edu

<sup>3</sup>Flow Science Inc. (USA)

<sup>4</sup>Dept. of Electrical Engineering, State University of New York at Buffalo (USA)

## ABSTRACT

Continuous flow bioseparators allow magnetic particles that are properly functionalized so that they get attached to dangerous pathogens, to be easily captured in a buffer solution. Specifically, the unique properties of magnetic particles enable their separation from blood, after fulfilling their role of pathogen capture, in a continuous process. However, the optimization of the process, i.e. achieving high magnetic particle recovery while minimizing blood loss or dilution and avoiding diffusion between fluid phases, remains a technological challenge. Therefore, in this study, we introduced a CFD-based Eulerian-Lagrangian approach using the commercial CFD software package *FLOW-3D* to model particle magnetophoresis in a two-phase continuous-flow microseparator where the particles were continuously separated from the blood stream and collected into a co-flowing buffer solution. A combination of mass transfer, magnetic and fluidic computational models were used to accurately describe the particle motion, along with any effects on the interface between phases and the diffusion of blood components to the buffer phase. A numerical CFD analysis was used to predict the particle-fluid transport, whereas an analytical approach is employed for the prediction of both the magnetic field generated by permanent magnets and the corresponding magnetic force on the particles. The parametric analysis focuses on the impact of different variables, such as flow rates, particle and magnet sizes and the viscosity of the fluid phases, on particle recovery. The model was also experimentally validated through fluorescence microscopy. The simulation data fits the experimental results within an absolute error of 15%. Overall, this computational analysis helps promote the fundamental understanding of the underlying phenomena while offering a powerful platform for the design of magnetophoretic components that can be integrated into lab-on-a-chip systems for bioseparation processes.

**Keywords:** magnetic particle separation, flow patterns, mass transfer, CFD modeling, two-phase liquid-liquid microfluidic systems, blood detoxification.

## 1. INTRODUCTION

In recent years, there has been a proliferation of applications of superparamagnetic beads in a diverse range of fields. Some of the most recent works have addressed the use of magnetic beads for the extracorporeal removal of toxic substances from blood [1-3], which can be considered the most conceivable treatment for different clinical conditions. Blood detoxification using magnetic beads is an extracorporeal process wherein the patient's blood is infused with magnetic materials with the ultimate goal of the selective removal of toxins while maintaining healthy functionality of blood constituents. Once the adsorption of the toxins onto the beads surface is completed, the magnetic separation stage takes place and the toxins are removed along with the material, leading to a toxin-free blood solution that returns to the circulatory system of the patient.

Numerous microfluidic magnetic separator designs have been proposed in the last years for carrying out the recovery of magnetic beads from different biological fluids, including blood [3]. The use of continuous-flow systems poses several advantages compared to batch magnetic separators [4]. However, the complexity of these systems is high and many design challenges, which need to be addressed, exist. Thus, the progress of this novel technology requires the following: (a) the complete capture of the magnetic bead-toxin complexes using appropriate nonuniform magnetic fields (i.e. those that exhibit a gradient in the field distribution) and (b) the control of the neighboring coflowing fluids (blood and buffer), without their intermixing inside the device. In this work, we introduce a combination of magnetic and fluidic computational models that describe the bead trajectory inside a symmetric microchannel under the influence of an external permanent magnet. The impact of different process variables and parameters – flow rates, bead and magnet dimensions and fluid viscosities – on both bead recovery and blood loss or dilution is quantified for the first time. This approach is well-suited for parametric analysis and optimization, thereby facilitating the development of novel microfluidic systems not only for blood detoxification processes but also for many other biomedical applications that involve two or more confined liquid phases.

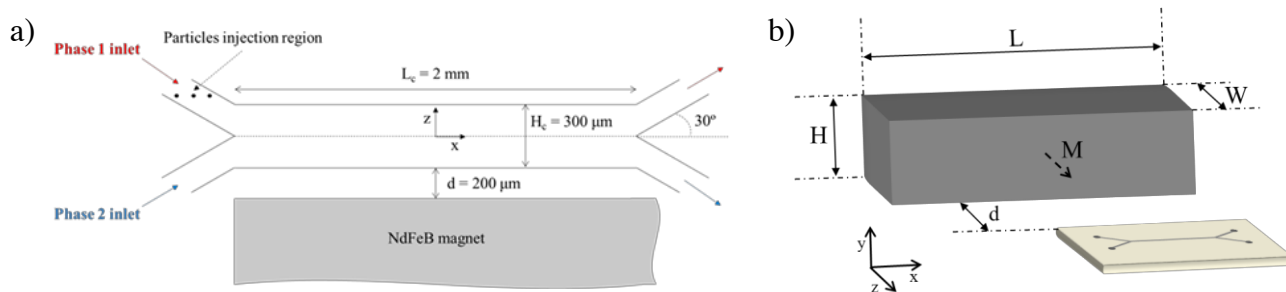


**Figure 1.** a) Schematic view of the design of the continuous-flow magnetophoretic separator; b) Magnet-channel system showing geometry and magnetization.

## 2. THEORY

The model was developed by customizing a commercial multiphysics CFD software program, **FLOW-3D** from Flow Science Inc. (ver11.2, [www.flow3d.com](http://www.flow3d.com)). The model for predicting the magnetophoretic particle transport inside the separator shown in **Figure 1** involves a CFD-based Eulerian-Lagrangian approach. The Lagrangian framework is used to model the bead dynamics, whereas the fluid transport, which is predicted by solving the Navier-Stokes equations, is calculated with an Eulerian approach.

The model is based on the following assumptions: (a) all fluids are Newtonian and incompressible (blood is assumed to follow a Newtonian rheology as it has been demonstrated to follow such behavior when the shear rate exceeds about  $100\text{ s}^{-1}$ ) [5], (b) the magnetic particles have a linear magnetization curve with saturation, (c) interparticle magnetic dipole-dipole coupling is negligible because of a low particle concentration, (d) the field sources are ideal 3D rare-earth permanent magnets, and (e) there are no other magnetic materials present in the computational domain that would otherwise perturb the magnetic field. This last assumption is important as it allows the use of analytical expressions for the magnetic field distribution and force. Thus, the need for numerical field predictions, which greatly simplifies the analysis and reduces simulation time, is eliminated.

According to the Lagrangian approach, particles are modelled as discrete units and the trajectory of each one is estimated by applying the classical Newtonian dynamics:

$$m_p \frac{d\mathbf{v}_p}{dt} = \sum \mathbf{F}_{\text{ext}} \quad (1)$$

where  $m_p$  and  $\mathbf{v}_p$  are the mass and velocity of the particle and  $\mathbf{F}_{\text{ext}}$  represents all external force vectors exerted on the particle. Although different force contributions act on the particles during separation, only the dominant magnetic ( $\mathbf{F}_{\text{mag}}$ ) and fluidic ( $\mathbf{F}_{\text{drag}}$ ) forces were considered in this work. Expressions for the magnetic and drag forces acting on a particle can be found in our published works [5-7].

## 3. EXPERIMENTAL METHODOLOGY

For the fluidic analysis, fluids with two different characteristics were pumped into the two inlets: a) Phase 1 - Fluorescein sodium salt solution (employed as a coloring agent to distinguish the phases), and b) Phase 2 - deionized water or a mixture of ethylene glycol in water 50% v/v, that exhibits a density and viscosity values similar to human blood ( $1050\text{ kg}\cdot\text{m}^{-3}$  and  $4.1\text{ cP}$  at  $20^\circ\text{C}$ ). For the mass transfer analysis, we employed a specific Phase 1 fluorescein solution ( $60\text{ mg}\cdot\text{L}^{-1}$ , diffusion coefficient for fluorescein in water:  $4.25\cdot 10^{-6}\text{ cm}^2\cdot\text{s}^{-1}$ ), whereas deionized water was pumped into the phase 2 inlet.

For the particle separation analysis, different rare-earth NdFeB magnets were chosen as the magnetic sources, with dimensions  $L\times H\times W$  (Fig. 1 b) equal to  $5\times 5\times 3$ ,  $8\times 8\times 4$  and  $10\times 5\times 3\text{ mm}^3$ , respectively. Finally, for the magnetic bead recovery analysis, we prepared aqueous solutions of fluorescent magnetic beads of two different sizes, i.e.  $2.29$  or  $4.9\text{ }\mu\text{m}$  in diameter at a constant concentration of  $0.1\text{ g}\cdot\text{L}^{-1}$ . To evaluate the influence of viscous biofluids on the bead recovery, bead solutions were prepared in ethylene glycol solutions 50% v/v.

For optimization purposes, a dimensionless number ( $J$ ), that takes into account all the key fluidic and magnetic variables and parameters, was calculated. More specifically, the  $J$  number describes the relation between magnetic (particle volume  $V_p$  and magnetization  $f(H_a)$ , magnetic field strength  $\mathbf{H}_a$  and gradient inside the channel  $\nabla\mathbf{H}_a$ ) and fluidic (particle size  $r_p$ , viscosity of the fluids  $\eta$  and inlet mean velocities  $v_{\text{mean}}$ ) variables that impact the process. Thus, the  $J$  number scales both the magnetic (in  $z$  direction) and drag (in  $x$  direction) forces on a particle located in the middle of our channel just above the magnet (this location was chosen because of the average values of the magnetic force acting at that point). The  $J$  number can be written as follows:

$$J = \frac{\overline{F_{\text{mag},z}}}{\overline{F_{\text{drag},x}}} \quad (2)$$

## 4. RESULTS AND DISCUSSION

### 4.1 Fluidic analysis

In Figs. 2 a) and 2 b), the flow patterns and mass transfer in the continuous-flow separator are analyzed in order to examine the flow conditions that lead to the complete separation of the fluids at the bioseparator outlets. Furthermore, we study the flow conditions that minimize the interdiffusion between streams.

The volumetric fraction occupied by both fluids (aqueous fluorescein-ethylene glycol solution) is presented in Fig. 2 a). The independent co-flow is achieved when the phases are introduced into the channel at different flow rates. In fact, when the fluids have different viscosity, the pressure drop developed along the channel length is different and phase separation is negatively affected. Thus, phase separation inside the device is optimized when the flow rates are tuned, so that the pressure drop for each fluid phase is the same, as presented in Fig. 2. Furthermore the experimental images are in agreement with our theoretical predictions as seen in Fig. 2.

We also analyzed the diffusion of fluorescein from phase 1 to phase 2 as a function of  $\gamma$  (ratio between residence and diffusion times). We observed that for  $\gamma$  values close to 1, the fluorescein has time to completely diffuse to phase 2. Nonetheless, keeping this value close to 0.01, as presented in Fig. 2 b), we could neglect fluorescein diffusion from phase 1 to phase 2. Furthermore, the fluorescence intensity at the lower outlet is not perceived from the experimental image. Thus, working with  $\gamma$  values of approximately 0.01, the diffusion of relatively small molecules (such as plasma electrolytes) and big macromolecules (blood proteins) can be considered negligible.

### 4.2 Magnetic bead separation

Regarding the magnetic recovery analysis, for flowrates between  $0.2\text{--}1.5\ \mu\text{L}\cdot\text{s}^{-1}$  and for the  $4.9\ \mu\text{m}$  beads, separation yields between 23 and 100% are obtained, depending on the magnet sizes (as presented in Figure 3 a), when aqueous phases are used. Because of the similarity of the magnetic fields generated by each magnet (400 mT in the magnet's surface and 50 mT in the microchannel), the magnetic forces exerted on the particles were also similar (0.25 nN in the chip's wall closest to the magnet and 0.2 nN in the upper wall) and therefore, particle recovery, being slightly higher for the highest magnet size.

On the other hand, the magnetic force acting on the particles decreases one magnitude order when  $2.29\ \mu\text{m}$  particles are used compared to the  $4.9\ \mu\text{m}$  ones (Fig. 3 b). However, the drag force is kept in the same magnitude order for both particle sizes. Therefore, the magnetic recovery of the smallest particles is considerably lower (20-80%) than for the highest ones.

Finally, when viscous phases are employed at the same flowrates, the magnetic recovery was greatly reduced. In this case, the use of low flow rates (around  $0.3\ \mu\text{L}\cdot\text{s}^{-1}$ ) is required in order to achieve an adequate separation from viscous biofluids. This flow rate value results in average velocity values of  $0.33\ \text{cm}\cdot\text{s}^{-1}$ , with residence times of around 0.6 s, which is still a small value to allow diffusion of blood macromolecules to the buffer stream. Therefore, for the separation of beads from viscous solutions such as blood, slower flow rates could be safely employed since the integrity of the biofluid will not be compromised. It should be noted that the experimental results are found to match theoretical predictions within an absolute error of 15%

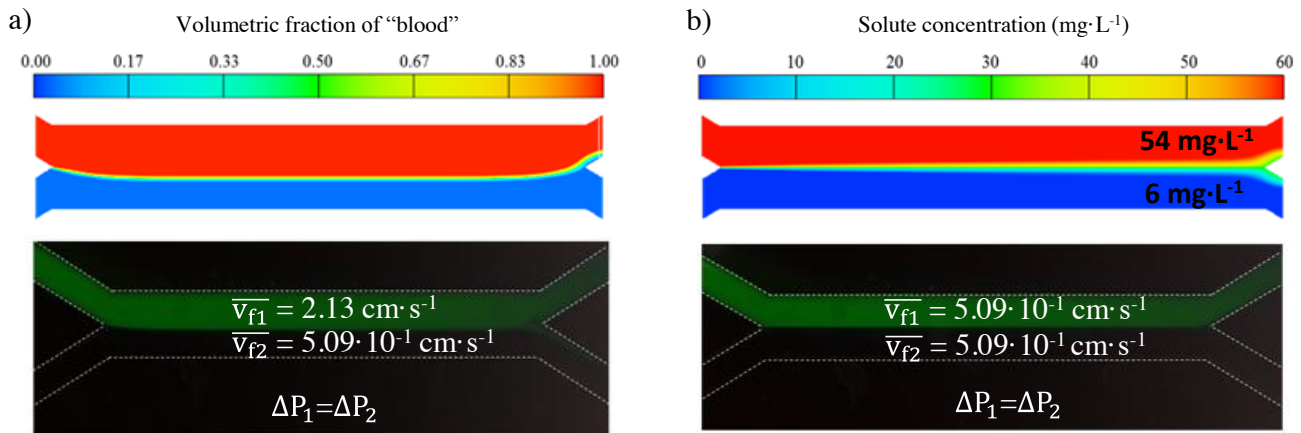


**Figure 2.** Fluid phase flow patterns and mass transfer. a) Simulation and experimental results of flow patterns of fluorescein (aqueous) and ethylene glycol ("blood") solutions when the pressure drop for both phases is ensured along the channel length. b) Fluorescein mass transfer by diffusion when the ratio ( $\gamma$ ) between the residence and the diffusion times is around 0.01.

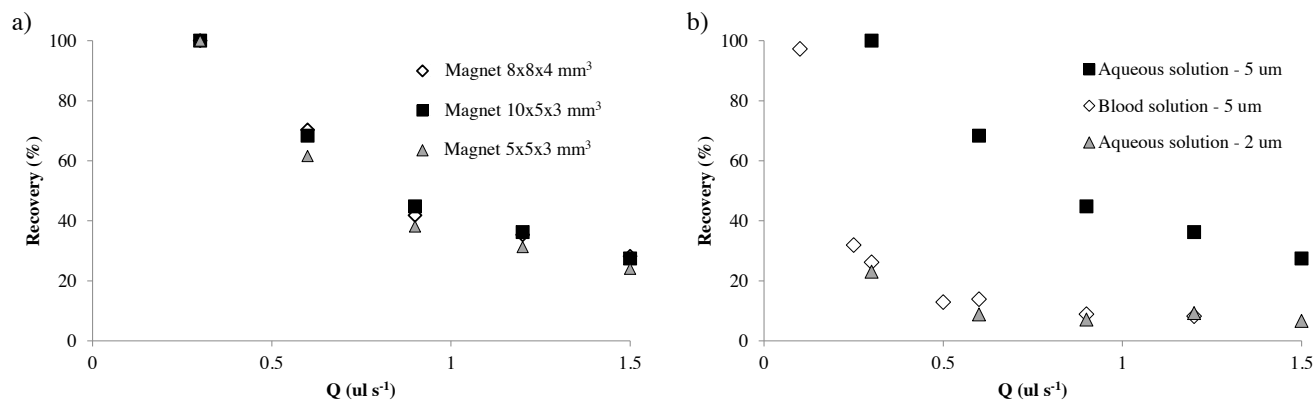


**Figure 3.** a) Influence of the magnet size on the magnetic bead recovery for the  $4.9 \mu\text{m}$  beads. b) Influence of both particle size and viscosity of the fluid phases on the bioseparator performance.

## 5 CONCLUSIONS

We have introduced a novel computational model for predicting and optimizing the process of magnetic bead separation from blood in a multiphase continuous-flow microdevice. The model takes into account dominant magnetic and hydrodynamic forces on the beads, as well as coupled bead-fluid interactions. Fluid flow (Navier-Stokes equations) and mass transfer (Fick's Law) between the coflowing fluids are solved numerically, while the magnetic force on the beads is predicted using analytical methods. The impact of different process variables and parameters – flow rates, bead and magnet dimensions and fluid viscosities – on both bead recovery and blood loss or dilution is quantified for the first time. The performance of the prototype device was characterized using fluorescence microscopy and the experimental results are found to match theoretical predictions within an absolute error of 15%. While the model is demonstrated here for analysis of a detoxification device, it can be readily adapted to a broad range of magnetically-enabled microfluidic applications, e.g. bioseparation, sorting and sensing.

## ACKNOWLEDGEMENTS

Financial support from the Spanish Ministry of Economy and Competitiveness under the projects CTQ2015-72364-EXP/AEI and CTQ2015-66078-R is acknowledged. J. Gómez-Pastora thanks the FPI postgraduate research grant (BES-2013-064415). C. González-Fernández thanks the Concepción Arenal postgraduate research grant from the University of Cantabria. E.P. Furlani acknowledges financial support from the U.S. National Science Foundation, through Award CBET-1337860.

## REFERENCES

- Herrmann, I. K.; Uner, M.; Koehler, F. M.; Hasler, M.; Roth-Z'Graggen, B.; Grass, R. N.; Ziegler, U.; Beck-Schimmer, B.; Stark, W. J. Blood Purification Using Functionalized Core/Shell Nanomagnets. *Small* **2010**, *6*, 1388–1392.
- Gómez-Pastora, J.; Bringas, E.; Lázaro-Díez, M.; Ramos-Vivas, J.; Ortiz, I. The Reverse of Controlled Release: Controlled Sequestration of Species and Biotoxins into Nanoparticles (NPs). In *Drug Delivery Systems*; Stroeve, P.; Mahmoudi, M., Eds.; World Scientific: New Jersey, 2017.
- Kang, J. H.; Super, M.; Yung, C. W.; Cooper, R. M.; Domansky, K.; Graveline, A. R.; Mammoto, T.; Berthet, J. B.; Tobin, H.; Cartwright, M. J.; et al. An Extracorporeal Blood-Cleansing Device for Sepsis Therapy. *Nat. Med.* **2014**, *20*, 1211–1216.
- Gómez-Pastora, J.; Xue, X.; Karampelas, I. H.; Bringas, E.; Furlani, E. P.; Ortiz, I. Analysis of Separators for Magnetic Beads Recovery: From Large Systems to Multifunctional Microdevices. *Sep. Purif. Technol.* **2017**, *172*, 16–31.
- Gómez-Pastora, J.; Karampelas, I. H.; Xue, X.; Bringas, E.; Furlani, E. P.; Ortiz, I. Magnetic Bead Separation from Flowing Blood in a Two-Phase Continuous-Flow Magnetophoretic Microdevice: Theoretical Analysis through Computational Fluid Dynamics Simulation. *J. Phys. Chem. C* **2017**, *121*, 7466–7477.
- Furlani, E. P.; Ng, K. C. Analytical Model of Magnetic Nanoparticle Transport and Capture in the Microvasculature. *Phys. Rev. E* **2006**, *73*, 1–10.
- Furlani, E. P. *Permanent Magnet and Electromechanical Devices; Materials, Analysis and Applications*; Academic Press: New York, 2001.